Development 133, 1477-1484 (2006) doi:10.1242/dev.02319

spn-F encodes a novel protein that affects oocyte patterning and bristle morphology in *Drosophila*

Uri Abdu[1,*], Dikla Bar[1] and Trudi Schüpbach[2]

The anteroposterior and dorsoventral axes of the *Drosophila* embryo are established during oogenesis through the activities of Gurken (Grk), a Tgfα-like protein, and the Epidermal growth factor receptor (Egfr). *spn-F* mutant females produce ventralized eggs similar to the phenotype produced by mutations in the *grk-Egfr* pathway. We found that the ventralization of the eggshell in *spn-F* mutants is due to defects in the localization and translation of *grk* mRNA during mid-oogenesis. Analysis of the microtubule network revealed defects in the organization of the microtubules around the oocyte nucleus. In addition, *spn-F* mutants have defective bristles. We cloned *spn-F* and found that it encodes a novel coiled-coil protein that localizes to the minus end of microtubules in the oocyte, and this localization requires the microtubule network and a *Dynein heavy chain* gene. We also show that Spn-F interacts directly with the Dynein light chain Ddlc-1. Our results show that we have identified a novel protein that affects oocyte axis determination and the organization of microtubules during *Drosophila* oogenesis.

KEY WORDS: *Drosophila*, Oogenesis, Microtubule, Bristle formation, *spn-F*

INTRODUCTION

The anteroposterior (AP) and dorsoventral (DV) axes of the *Drosophila* embryo are established during oogenesis by communication between the oocyte and the surrounding follicle cells (Schüpbach, 1987; Ruohola-Baker et al., 1994). This communication is mediated by a single signaling system involving the *gurken* (*grk*) and *Epidermal growth factor receptor* (*Egfr*) genes (Gonzalez-Reyes et al., 1995; Roth et al., 1995). *grk* encodes a Tgfα-like protein that is expressed in the germline and is secreted from the oocyte (Neuman-Silberberg and Schüpbach, 1993; Neuman-Silberberg and Schüpbach, 1996). Egfr is expressed throughout the follicular epithelium (Kammermeyer and Wadsworth, 1987; Sapir et al., 1998), where it acts as a receptor for Grk. In earlier stages of oogenesis, localized activation of Egfr at one end of the egg chamber establishes posterior follicle cell fates. The follicle cells signal back to the oocyte and this initiates the formation of the embryonic AP axis (Gonzalez-Reyes et al., 1995; Roth et al., 1995). After the oocyte nucleus has shifted to one side of the egg chamber at stage 8, *grk* RNA accumulates in a crescent close to the nucleus, and the resulting Gurken protein activates the receptor on one side of the egg chamber to establish dorsal follicle-cell fates. The production and localization of *grk* RNA and protein within the oocyte is tightly regulated at several levels (for a review, see Nilson and Schüpbach, 1999).

The asymmetric localization of *grk* mRNA within the developing egg chamber during mid-oogenesis requires a network of polarized microtubules (MTs). Before stage 7, a microtubule-organizing center (MTOC) is located at the posterior of the oocyte, as revealed by the localization of the unconventional kinesin Nod fused to β-galactosidase (Nod:β-gal) (Clark et al., 1997). The first *grk* signaling event leads to a repolarization of the oocyte MTs and the migration of the oocyte nucleus to the dorsoanterior corner of the oocyte (Gonzalez-Reyes et al., 1995; Roth et al., 1995). During stage 8, the posterior MTOC disassembles and a diffuse MTOC forms at the anterior. The anterior MTOC has been visualized by Nod:β-gal (Clark et al., 1997), Centrosomin (Li and Kaufman, 1996) and the MT-nucleating factors, γ-Tubulin at 37C (γTub37C) and the γ-Tubulin ring complex protein 75 (Grip75; previously known as Dgrip75) (Schnorrer et al., 2002). Injection of fluorescent *grk* mRNA into living oocytes revealed that the mRNA is assembled into particles that move in two distinct steps along two different MT arrays, first toward the anterior and then, after an apparent turn, dorsally toward the oocyte nucleus (MacDougall et al., 2003). High-resolution imaging of Tau-GFP (MacDougall et al., 2003; Januschke et al., 2002) and Nod:β-gal distribution in the oocyte suggests that there is a distinct network of MTs that are specifically associated with the oocyte nucleus, and these MTs are responsible for the second step in *grk* RNA localization. Moreover, recent work suggested that repositioning of the nucleus and its tightly associated centrosome could control MT reorganization in the *Drosophila* oocyte (Januschke et al., 2006). However, the precise nature and regulatory mechanisms that establish these oocyte nucleus-associated MTs is still unknown.

To further understand the role of MTs in *grk* RNA localization, we molecularly analyzed the *spn-F* locus. *spn-F* was first identified as a maternal effect mutation that affects the DV polarity of the eggshell (Tearle and Nüsslein-Volhard, 1987). We found that the ventralization of the eggshell in *spn-F* mutants is due to defects in the localization and translation of *grk* mRNA during mid-oogenesis. Moreover, we found that, in addition to the maternal effect, *spn-F* affects the development of the bristles of the adult fly. We show that transport toward the minus end of the MTs is affected in *spn-F* mutants, predominantly in the subset of MTs that are required for the transport of *grk* RNA from the anterior to the dorsal side of the oocyte towards the nucleus. We cloned *spn-F* and found that it encodes a novel coiled-coil protein that localizes to the minus end of MTs in the oocyte and in a punctate pattern in the nurse cells. Treatment of ovaries with the MT-depolymerization drug colcemid led to abrogation of Spn-F localization at the minus end of the MT and to higher accumulation of the protein in the nurse cells. We show

[1]Department of Life Sciences and the National Institute for Biotechnology in the Negev, Ben-Gurion University, Beer-Sheva 84105, Israel. [2]Howard Hughes Medical Institute, Department of Molecular Biology, Princeton University, Princeton, NJ 08544, USA.

*Author for correspondence (e-mail: abdu@bgu.ac.il)

Accepted 9 February 2006

that Spn-F interacts directly with the minus end-directed, motor-protein subunit Dynein light chain. Moreover, Spn-F localization to the minus end of the MT requires a *Dynein heavy chain* (*Dhc*) gene. Taken together, our results identify a novel protein that is involved in the organization of MTs in the oocyte during mid-oogenesis stages.

MATERIALS AND METHODS

Fly strains

Oregon-R was used as a wild-type control. The following mutant or transgenic flies were used: *spn-F*^{234}, *Df(3R)tll-g*, *Df(3R)tll-e*, *Act5C-GAL4* (*Drosophila* Stock Center, Bloomington), *Df(3R)A177der20* and *Df(3R)A177der21*^{38}, *Dhc*$^{6-6}$, *Dhc*$^{6-12}$ (Gepner et al., 1996), *spn-F*^{2} (Drosophila Stock Center, Szeged; originally designated *l(3)s113003*). The chromosome designated *l(3)s113003* failed to complement the *spn-F* bristle and ovarian phenotypes. It had been suggested that this line carried two P-element insertions: the first was mapped to 62E by in situ hybridization and the second was uncovered by *Df(3R)A177der21* [the second insertion site appears to be a second site mutation where a P-element is no longer associated with the semi-lethality (Deak et al., 1997)]. Indeed, recombination allowed us to isolate a viable stock containing the *spn-F*^{2} mutation. We used the kinesin β-Gal insertion line KZ503 and the Nod-β-Gal insertion line *NZ143.2* (Clark et al., 1997), as well as Tau-GFP (Micklem et al., 1997). Germline clones were generated using the ovoD-FLP technique and the FRT82B (3R) (Chou and Perrimon, 1992). CG12114 was expressed in the ovary using the *nanos*-Gal4-VP16 expression system (Van Doren et al., 1998). The balancer chromosomes used in this study, as well as the marker mutations, have been described previously (see Lindsley and Zimm, 1992) (see also FlyBase, http://flybase.bio.indiana.edu).

Rescue construct

The entire coding sequence of *CG12214* was amplified by PCR from EST (LD01470), using modified primers to create a *Kpn*I restriction site at the 5′ end and a *Not*I site at the 3′ end. The PCR product was then cloned into pUASp. P-element-mediated germ-line transformation of this construct was carried out according to standard protocols (Spradling and Rubin, 1982).

Sequencing of mutant alleles

Genomic DNA was prepared from flies of the genotype *spn-F*/spn-F** according to standard procedures (Sambrook et al., 1989). The coding region was sequenced and the sequences were compared with the wild-type genomic sequence of the parental chromosomes using the MacVector (Kodak/IBI) program.

Generation of anti-Spn-F (CG12114) monoclonal and polyclonal antibodies

The entire open-reading frame of CG12114 was cloned into pGEX-2T (Pharmacia). The fusion protein was overexpressed in *Escherichia coli* and the inclusion bodies were purified using a standard protocol (Sambrook et al., 1989). The CG12114 monoclonal antibodies were prepared by the Princeton monoclonal facility and the polyclonal antibodies were raised in rabbits by PRF&L Company, using the purified inclusion bodies as antigen.

In situ hybridization and antibody staining

RNA in situ hybridization on ovaries was performed using digoxigenin-labeled probes according to standard protocols (Roth and Schüpbach, 1994). Antibody staining of ovaries was carried out as described (Queenan et al., 1999), using mouse anti-Grk (1:10), mouse anti-CG12114 (1:10; clones 8C10 and 3F1), rabbit anti-Oskar (1:500; kindly provided by P. MacDonald, University of Texas), mouse anti-α-tubulin (1:250; Sigma), rabbit anti-β-Gal (1:1000; Promega), rabbit anti Centrosomin (1:500) (Heuer and Kaufman, 1995) (kindly provided by T. Kaufman). The secondary antibodies Alexa Fluor-488 goat anti-rabbit IgG and Alexa Fluor-568 goat anti-mouse IgG (Molecular Probes) were used at a dilution of 1:1000. For experiments involving α-tubulin and Tau-GFP staining, ovaries were fixed in 4% paraformaldehyde in PBS+0.1% Triton X-100 for 20 minutes at room temperature and the ovaries were then kept at room temperature to ensure that the MTs did not depolymerize. DNA was stained with Hoechst (Molecular Probes) at a dilution of 1:10,000. Wheat Germ Agglutinin (WGA-633, Molecular Probes, conjugated to Alexa Fluor-633) was used at a dilution of 1:500 for 1 hour at room temperature. MT detection was carried out as described (Januschke et al., 2006). Briefly, ovaries were incubated in BRB80 buffer [80 mmol/l PIPES (pH 6.8), 1 mmol/l $MgCl_2$, 1 mmol/l EGTA], containing 1% Triton X-100 (BRB-80-T) for 1 hour at 25°C without agitation. Then ovaries were fixed in MeOH at –20°C for 15 minutes, rehydrated for 15 hours at 4°C in PBS 0.1% Tween, then blocked for 1 hour in PBS 0.1% Tween containing 2% (w/v) bovine serum albumin (BSA) before incubation with primary antibody overnight.

Drug treatment

Drugs were fed to 2- to 3-day-old adult females in a yeast paste, following a one-hour starvation. Colchicine (Sigma) was used at a concentration of 25 μg/ml for periods of 24 hours. Antibody staining of the ovaries was carried out as described above.

Scanning electron microscopy

Scanning electron microscopy was performed in the Materials Institute of Princeton University on a Philips XL 30 PEG-SEM. Adult *Drosophila* were fixed in 70% ethanol overnight and dehydrated through a series of 10-minute washes in 95% ethanol, 100% ethanol and acetone. The flies were dried with Tetramethylsilane Ted-Pella for 10 minutes in capped tubes. The TMS was allowed to evaporate, samples were mounted upon stubs and sputter coated with gold.

GST pull-down assays

Expression of GST-Ddlc was performed as described previously (Schnorrer et al., 2000). The CG12114 was cloned into pHIS and protein induction performed overnight at 15°C. The recombinant protein samples were purified in phosphate-buffered saline (PBS). A 10-μl bed volume of glutathione-Sepharose resin was added to 30 μg of GST-Ddlc or GST alone, and the mixture was incubated on ice for 30 minutes before adding purified Spn-F. The mixture was incubated on ice overnight. The resin was then washed four times with 500 μλ PBS. The bound protein was eluted from the resin with 30 μl of Laemmli buffer and boiled for 5 minutes. After centrifugation, the supernatant was subjected to 15% SDS-PAGE followed by staining with Coomassie brilliant blue-G250.

For GST and ovary extract pull downs (with GSH–Sepharose, Pharmacia) equal amounts of ovary extracts were lysed, incubated and washed with 50 mM HEPES (pH 7.5), 150 mM NaCl, 1% NP-40, 10% glycerol and a cocktail of a complete protease inhibitor (Roche). Recombinant GST or GST-Ddlc protein (~5 μg) was incubated with ovarian extracts for up to 4 hours at 4°C; the beads were washed four times with lysis buffer and eluted in Laemmli buffer. Western blots were performed using polyclonal anti-Spn-F antibodies at a 1:1000 dilution.

RESULTS

Spn-F affects the pattern of the eggshell and the embryo

Females mutant for *spn-F*^{234} produce a ventralized eggshell (Tearle and Nüsslein-Volhard, 1987) (Fig. 1A,B, Table 1). A fraction of the eggs are fertilized and the embryos that form inside have a variety of pattern abnormalities (Fig. 1). Apart from ventralized embryos that resemble embryos produced by weak *gurken* mutations, some bicaudal embryos are found inside the eggs, ranging from embryos with the typical reduced head skeleton to rare symmetrical bicaudals with several abdominal segments in mirror image symmetry (Fig. 1C,D), and Filzkoerper and telson at both ends. We analyzed the localization of Osk protein, whose posterior concentration depends on endogenous *kinesin heavy chain* function (Brendza et al., 2002). The localization of *oskar* RNA in *spn-F* mutants is similar to that observed in wild type (data not shown); however, we found that the posterior association of Oskar protein with the cortex in *spn-F* stage 10 oocytes is not as tight as in wild type (Fig. 1E,F).

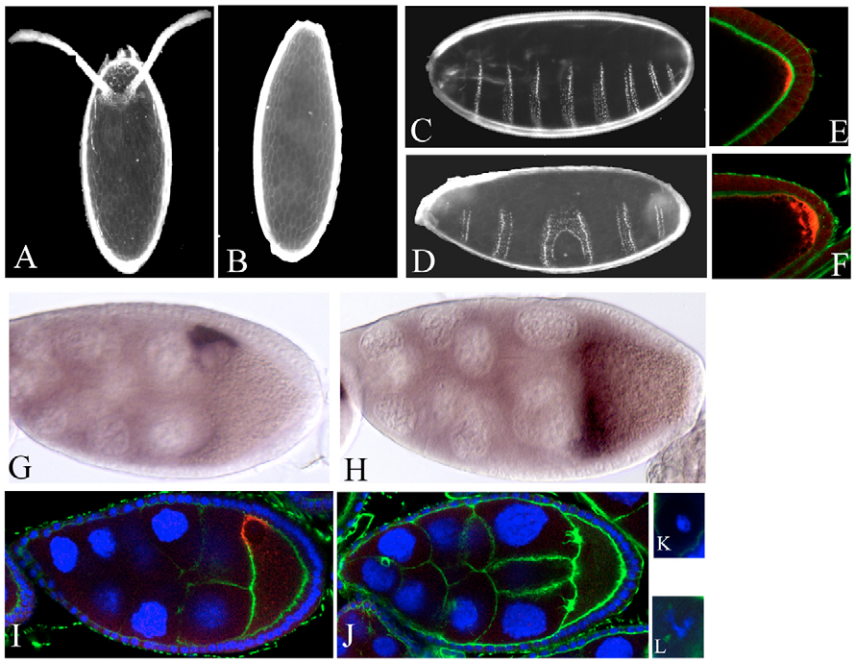

Fig. 1. DV and AP patterning defects in *spn-F* mutants. (**A**,**B**) Eggshells from *spn-F* mutant females. (A) Wild-type eggshell; (B) strongly ventralized egg shell. (**C**,**D**) Wild type embryo (C); bicaudal embryo in egg of *spn-F* mutant (D). Only a few percent of *spn-F* eggs (1-3%, depending on background) gave rise to bicaudal embryos. (**E**,**F**) Oskar protein localization at the posterior pole of stage 10 wild-type (E) and *spn-F* (F) egg chambers (Oskar, red; cortical Actin, green). The Oskar protein is not tightly localized to the posterior pole in the mutant. (**G**,**H**) *grk* RNA in situ localization in stage 9 wild-type (G) and *spn-F* (H) egg chambers. In most mutant egg chambers at stages 9-10, *grk* RNA forms a broad, fuzzy band around the anterior. (**I**,**J**) Grk protein expression in stage 9 wild-type (I) and *spn-F* (J) egg chambers, with Grk in red, cortical actin detected with Phalloidin in green and DNA in blue. Grk protein is strongly reduced in the mutant egg chambers. (**K**,**L**) Defects in oocyte nuclear morphology in *spn-F* (DNA, blue). In wild-type egg chambers (K), the DNA in the oocyte is condensed into a tight sphere. In *spn-F* egg chambers (L), the DNA appears fragmented.

spn-F affects oocyte nuclear morphology, and *grk* RNA localization and protein accumulation

The ventralization of eggshells in the *spn-F* mutant is similar to the phenotype produced by mutations in the *grk-Egfr* pathway. As *spn-F* is required in the germline (data not shown), we examined the effect of *spn-F* mutations on the localization and expression of *grk* RNA. In wild-type ovaries, *grk* RNA accumulates in the oocyte during earlier stages of oogenesis. In mid-oogenesis, it is localized within the oocyte, first transiently in an anterior-cortical ring (stage 8 and early stage 9), and then to a dorsoanterior domain in the cytoplasm directly overlying the oocyte nucleus (stages 9 and 10, Fig. 1G). In *spn-F* mutant ovaries, *grk* RNA is correctly localized to the oocyte in early stages. However, in mid-oogenesis, in the majority of stage 9 and 10 mutant egg chambers, *grk* RNA is found in a diffuse ring at the anterior margin of the oocyte rather than above the oocyte nucleus (Fig. 1H). In addition to the effect of *spn-F* on *grk* RNA localization, the accumulation of Grk protein is also affected. In wild-type egg chambers, Grk is restricted to the oocyte, and in mid-oogenesis it is localized to the dorsoanterior corner of the oocyte, similar to the RNA (Neuman-Silberberg and Schüpbach, 1996) (Fig. 1I). In *spn-F* mutant ovaries, Grk is also restricted to the oocyte; however, the levels of Grk are variably reduced throughout oogenesis, and in 67% of the stage 9 egg chambers Grk protein was undetectable (Fig. 1J). The DNA within the oocyte nucleus is often fragmented or thread-like in appearance (Fig. 1L), similar to the phenotype produced by spindle class genes (e.g. *okra*, *spn-A*, *spn-B*, *spn-D*) (Gonzalez-Reyes et al., 1997; Ghabrial et al., 1998; Abdu et al., 2003; Staeva-Vieira et al., 2003).

spn-F does not act through the meiotic checkpoint

Several of the spindle class genes, which are characterized by a variable eggshell ventralization phenotype, were previously found to encode proteins with homology to known DNA repair enzymes, and were shown to be required for the repair of recombination-induced, double-strand DNA breaks during *Drosophila* oogenesis (Ghabrial et al., 1998; Abdu et al., 2003; Staeva-Vieira et al., 2003). *Spindle A*, *B*, *C* and *D* patterning defects can be suppressed; for instance, by blocking the formation of double-strand DNA breaks during meiosis using mutations in *mei-W68* (Ghabrial and Schüpbach, 1999), or by eliminating the checkpoint by using mutation in the checkpoint genes *mei-41* and *DmChk2* (*lok* – FlyBase) (Ghabrial and Schüpbach, 1999; Abdu et al., 2002). To determine whether the ovarian phenotype in *spn-F* is also due to unrepaired double-strand DNA breaks, flies double mutant for *mei-W68* or *DmChk2* and *spn-F* were generated. Our results showed that neither ventralization nor the defects in the appearance of the DNA within the oocyte nuclei of *spn-F* are suppressed by *mei-W68* or *DmChk2* (data not shown). These results strongly suggest that *spn-F* is not involved in the repair of double-strand DNA breaks during meiosis. The DV patterning defects of *spn-F* mutants therefore appear to arise by a mechanism that operates either downstream or independently of the meiotic checkpoint.

Bristle defects in *spn-F* mutants

In contrast to the other spindle class genes, *spn-F* also affects the development of the bristles (Fig. 2). When compared with wild type, *spn-F* mutants have considerably shorter and thicker bristles.

Table 1. Relative percentage of the different ventralized eggshell phenotypes found in *spn-F* mutants

Genotype	Class 1 – similar to wild type	Class 2 – appendages fused at base	Class 3 – single appendage	Class 4 – no appendage
$spnF^{1}$	4%	7%	9%	80%
$spnF^{1}$/Df	6%	5%	10%	79%
$spnF^{2}$	3%	8%	5%	84%
$spnF^{2}$/Df	7%	1%	4%	88%

The classification of eggshell ventralization is based on that of Ghabrial et al. (Ghabrial et al., 1998).
The deficiency *Df(3R)tll-e* (Df) was used in these experiments.

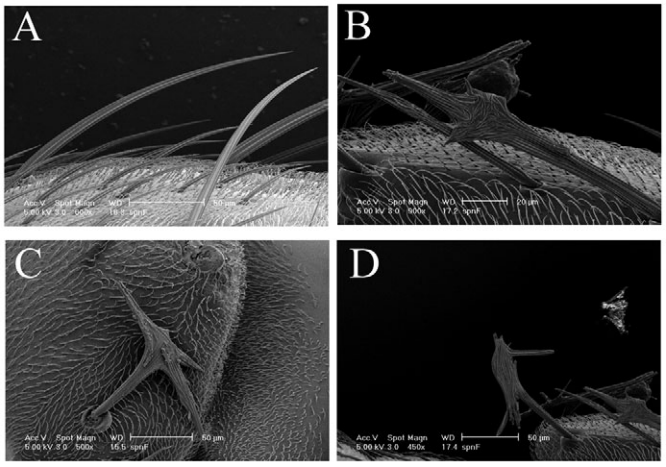

Fig. 2. Scanning electron micrographs of wild-type and *spn-F* mutant thorax bristles. (**A-D**) Wild-type bristles (A) are long and characterized by a thin and pointy tip, whereas *spn-F* mutant bristles (B-D) show thickening and branching, and are shorter than wild-type bristles.

Scanning electron micrographs of *spn-F* bristles showed that, in addition to the aberrant length and width, the morphology of *spn-F* bristles was altered; the *spn-F* bristles do not have finely tapered ends (Fig. 2B), and, in some extreme cases, the direction of bristle growth at some points along the bristle shaft is altered (Fig. 2C,D).

Actin and microtubule network in *spn-F* mutant ovaries

Because *spn-F* mutants affect the formation of the bristles and also the localization of *grk* RNA, we investigated whether the actin and/or the MT network are altered during oogenesis. To analyze the organization of the MT network in *spn-F* mutant egg chambers, we used two different markers, α-tubulin staining and localization of Tau-GFP, which labels MTs (Micklem et al., 1997) (Fig. 3). In wild-type egg chambers at early stages, we found that MTs are equally distributed in the oocyte cytoplasm (Fig. 3A). However, in *spn-F* early stages, the α-tubulin accumulated abnormally around the oocyte nuclear membrane (Fig. 3B). In wild-type stage 9 egg chambers, α-tubulin is enriched at the anterior region of the oocyte with a slightly higher accumulation around the oocyte nucleus (Fig. 3C). In *spn-F* stage 9 egg chambers, α-tubulin is abnormally associating with the oocyte nuclear periphery (Fig. 3D). The oocyte nucleus does, however, move normally to the dorsoanterior corner in the mutant egg chambers. Using Tau-GFP in stages 6-9 egg chambers (Fig. 3E-H), we observed that, in early stages in wild type and mutants, MTs were uniformly seen in the oocyte cytoplasm (Fig. 3E,F), whereas, at stage 9 of oogenesis, the MTs in both wild type and mutants were most abundant at the anterior margin of the oocyte and gradually diminished in concentration towards the posterior pole, as has been previously reported (Micklem et al., 1997) (Fig. 3E-H). In living specimens, using Tau-GFP at a higher magnification and resolution, it had been shown that, in wild-type egg chambers, a highly conserved array of MTs exists at the anterior of the oocyte and that this anterior array of MTs forms a basket around the oocyte nucleus (MacDougall et al., 2003). In GFP antibody-stained *spn-F* mutant egg chambers at stage 9, the Tau-GFP fusion protein accumulated abnormally in discrete 'dots' around the oocyte nucleus, similar to as was observed with the α-tubulin staining (Fig. 3B,D).

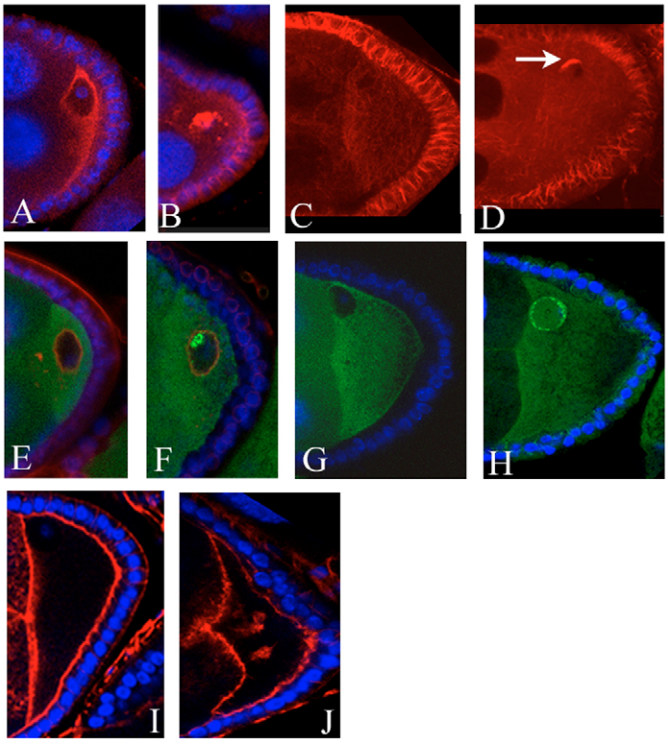

Fig. 3. Actin cytoskeleton organization and α-tubulin staining and Tau-GFP localization in wild-type and *spn-F* ovaries. (A,C,E,G,I) Wild-type egg chambers; (B,D,F,H,J) *spn-F* egg chambers. (**A**,**B**) Young egg chambers. α-tubulin, red; DNA, blue. (**C**,**D**) Stage 9 egg chambers. α-tubulin, red. Abnormal aggregates of tubulin are seen at the nuclear periphery in the mutant egg chambers (arrow in D). (**E**,**F**) Abnormal accumulation of Tau-GFP is visible, associated with the mutant oocyte nucleus. Tau-GFP, green; DNA, blue; nuclear membrane, red. (**G**,**H**) Tau-GFP forms a gradient from anterior to posterior at stage 9 in both wild type and mutant; however, an abnormal accumulation of Tau-GFP occurs at the oocyte nuclear membrane in the mutant. Tau-GFP, green; DNA, blue. (**I**,**J**) Abnormal clumps of actin can be seen in the mutant egg chamber (J), compared with wild type (I). Rhodamine-phalloidin staining, red; DNA, blue.

To examine the actin network, ovaries were stained with Rhodamine-conjugated phalloidin (Fig. 3I,J). In wild-type stage 8-9 egg chambers, most actin was uniformly and evenly distributed at the cortical surface (Fig. 3I); however, in 60% of *spn-F* mutant egg chambers, small irregularly shaped actin aggregates and actin clumps along the anterior ring below the actin-rich cortical layer were observed (Fig. 3J).

As a next step, we investigated the function and polarity of the MTs in *spn-F* mutant ovaries. First, the transport to the posterior pole of the oocyte was analyzed using the MT plus-end marker kin:β-gal (Clark et al., 1997). We found that kin:β-gal localization in *spn-F* mutants is similar to that observed in wild-type stage 9 egg chambers (Fig. 4A), in that the fusion protein is concentrated at the posterior end of the oocyte (Fig. 4B).

To analyze transport to the anterior pole, we used the MT minus-end marker Nod:β-gal (Clark et al., 1997). In wild-type stage 6 egg chambers, Nod:β-gal is concentrated at the posterior cortex of the oocyte (Fig. 4C). By stage 8, the protein is no longer detectable at the posterior of the oocyte but instead concentrates along the anterior cortex of the oocyte with highest accumulation flanking the oocyte nucleus (Fig. 4E). In *spn-F* mutant ovaries, neither the

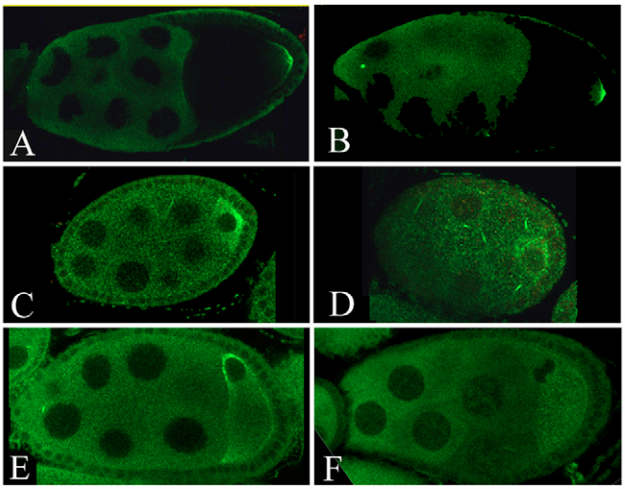

Fig. 4. kin:β-Gal and Nod:β-Gal localization in wild-type and *spn-F* egg chambers. (A,C,E) Wild-type egg chambers; (B,D,F) *spn-F* egg chambers; (C,D) stage 6 egg chambers; (E,F) stage 8 egg chambers. (**A**,**B**) kin:β-Gal localization (green). The localization to the posterior pole appears normal in the mutant egg chambers. (**C-F**) Nod:β-Gal localization (green). The localization of Nod:β-Gal appears less pronounced in the posterior in the stage 6 mutant egg chamber, and less concentrated around the oocyte nucleus in the stage 8 mutant than in wild type.

early posterior localization (Fig. 4D) nor the anterior ring localization in mid-oogenesis (Fig. 4F) are detected. These results indicate that transport to the minus end of the MTs or some aspect of anchoring cargoes to the MT network is not functioning properly in *spn-F* mutant egg chambers. To assay transport to the minus end of the MTs in the anterior ring during mid-oogenesis versus transport to the dorsoanterior corner of oocyte, we analyzed the localization of *bicoid*, *encore* (Fig. 5) and *fs(1)K10* RNA (data not shown), which all accumulate in an anterior ring, but are not further localized to the dorsal corner. We found that the localization of these RNAs in *spn-F* mutants is similar to that observed in wild type. We also found that Centrosomin, a MTOC component that marks MT minus ends (Li and Kaufman, 1996), is localized to the anterior ring of the oocyte in *spn-F* mutants, as in wild type (data not shown).

Molecular characterization of the *spn-F* locus

spn-F^{234} had been mapped to position 3-100 on chromosome 3R. We used chromosomal deficiencies to show that *spn-F*^{234} is uncovered by *Df(3R)tll-e* and *Df(3R)A177der21*, but not by *Df(3R)tll-g* and *Df(3R)A177der20*, indicating that *spn-F* is located between 100B1-100B9. To identify additional *spn-F* alleles, we crossed a set of P-element lines (Deak et al., 1997) that were initially mapped to this region to *spn-F*^{234}. One of the lines, *l(3)s113003* failed to complement the *spn-F* bristle and ovarian phenotypes. After we recombined this insertion away from a second insertion on the same chromosome (see Materials and methods), we were able to obtain a homozygous viable line that contained a second *spn-F* allele (*spn-F*^{2}). Both hemizygous and homozygous *spn-F*^{2} individuals are female sterile and show bristle defects similar to those observed in *spn-F*^{234}. We also found that there was no difference in the severity of DV defects of the eggshell between the hemizygous *spn-F*^{234} and *spn-F*^{2}, suggesting that both alleles are genetically null (Table 1).

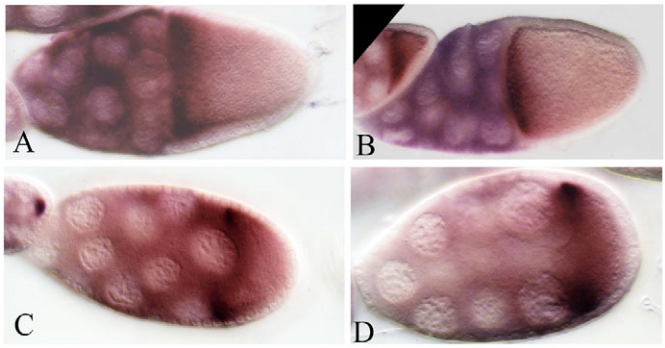

Fig. 5. *bcd* and *encore* RNA distribution in wild-type and *spn-F* ovaries. (A-D) *bcd* (A,B) and *encore* (C,D) mRNA in wild-type (A,C) and *spn-F* (B,D) egg chambers. The localization of these anterior RNAs appears normal in the mutant egg chambers.

Databank searches of region 100B1-100B9 revealed two likely candidate genes for *spn-F*. We sequenced both the *bottleneck* gene and *CG12114* in *spn-F*^{234} homozygotes, and found a nonsense mutation in *CG12114* at base pair 178 of its mRNA that results in a truncation of the predicted protein after amino acid 59. In *spn-F*^{2}, there is a 67-nucleotide deletion starting from nucleotide 726.

To demonstrate that these mutations in the *CG12114* gene are responsible for the defects observed in *spn-F* mutants, we expressed the entire *CG12114* open reading frame in the germline under UAS control, using a *nanos*-Gal4 driver line in the *spn-F*^{234} and *spn-F*^{2} mutant backgrounds, and found that this transgene fully rescues the female sterility (data not shown). Also, expressing *CG12114* using an actin-Gal4 driver rescued both the female sterility and the bristle defects. These results verify that *spn-F* indeed corresponds to the *CG12114* gene.

Blast searches of protein databases identify proteins in *Drosophila pseudoobscura* (GA11408; 70% identity and 78% similarity) and in *Anopheles gambiae* (GenBank number: XP_311294; 34% identity and 49% similarity) as the proteins most closely related to CG12114. From sequence analysis, the *spn-F* gene is predicted to encode a 40 kDa protein with coiled-coil domains between amino acids 32-114 and 210-243. No homologous protein has been found in the databases outside the Dipteran species mentioned above.

Spn-F protein is localized to the minus end of the microtubule and interacts with the Dynein light chain Ddlc-1 (Cut up)

To analyze the intracellular localization of Spn-F, we generated monoclonal antibodies against the *CG12114*-encoded protein (Fig. 6). In wild-type ovaries, during early stages of oogenesis, Spn-F protein is localized to the posterior pole of the oocyte (Fig. 6A); in later stages Spn-F becomes localized to the anterior margin, with higher accumulation around the oocyte nucleus (Fig. 6B). These results strongly suggest that Spn-F is localized to the minus end of the MTs in the oocyte. We also found that, in the nurse cells, Spn-F is found in a punctuate pattern (Fig. 6B). The antibody is specific for Spn-F, as such staining was not observed in *spn-F* mutant ovaries.

We next investigated the role of the MT network in Spn-F localization during oogenesis. Treatment of *Drosophil*a females with colcemid, a MT depolymerizing drug, simultaneously affects all MTs in the oocyte (Pokrywka and Stephenson, 1995). We found that treatment of ovaries with colcemid abrogates Spn-F localization at the minus end of the MTs both during early (data not shown) and mid-oogenesis (Fig. 6C). Moreover, we found that in colcemid-

treated ovaries, a more punctate distribution of Spn-F protein accumulated in the nurse cells when compared with wild-type ovaries (Fig. 6C). These results suggest that Spn-F is transported from the nurse cells to the oocyte via the MT network, and requires MTs for its localization to the posterior in early oocytes, and to the anterior in older oocytes.

In a two-hybrid-based, protein-interaction map of the fly proteome, several proteins were found to interact with Spn-F, among these, although with somewhat low confidence, is *cut up*, which encodes a Dynein light chain (Ddlc) (Giot et al., 2003). Ddlc is a highly conserved light-chain subunit of cytoplasmic Dynein, a MT minus-end motor protein that is thought to play a fundamental role in both the assembly of the motor complex and the recruitment of cargo. To investigate the direct association of Spn-F with Ddlc-1, a GST pull-down assay was conducted. First, recombinant GST alone (Fig. 6E, lane 1), GST-Ddlc (Fig. 6E, lane 2) and His tagged-Spn-F (Fig. 6E, lane 3) proteins were purified and analyzed by gel electrophoresis. Next, GST-Ddlc-1 bound to GSH-agarose (Fig. 6E, lane 4) or GST bound to GSH-agarose (Fig. 6E, lane 5) was incubated with purified Spn-F protein and a pull-down assay was performed. We found that Spn-F binds efficiently to GST-Ddlc-1 (Fig. 6E, lane 4), but not to GST alone (Fig. 6E, lane 5) or to any of the other GST-fusion proteins tested (data not shown).

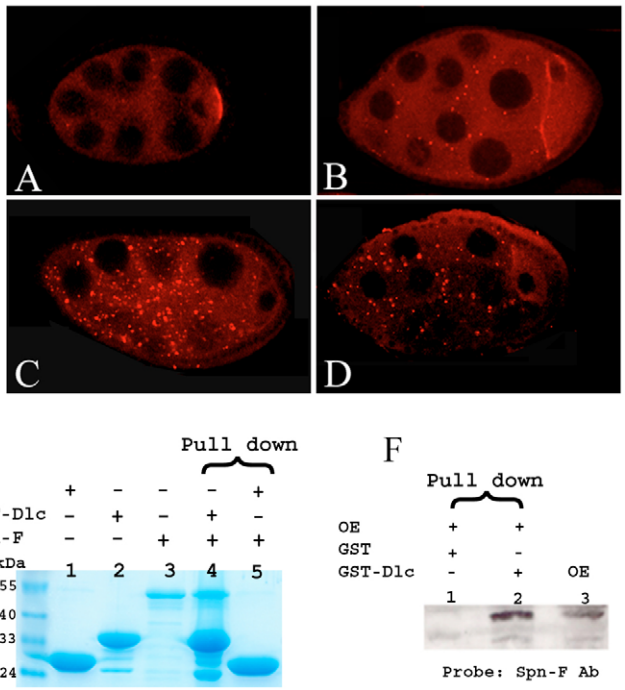

Fig. 6. Intracellular localization of Spn-F protein in *Drosophila* ovaries and its association with Dynein light chain in vitro. (**A-D**) Spn-F protein (red) accumulates at the posterior pole in egg chambers until stage 6 (A), and accumulates at the anterior cortex after stage 8 (B, stage 9 egg chamber) and also in a punctate pattern in the nurse cells. (C) In a colcemid-treated egg chamber, Spn-F protein does not localize to the anterior cortex and a more punctate distribution of Spn-F is detected in the nurse cells. (D) In egg chambers from *Dynein heavy chain* mutant flies, Spn-F protein does not localize significantly to the anterior cortex and a more punctate distribution in of Spn-F is detected in the nurse cells. (**E**) GST pull-down assay for the in vitro binding of His-Spn-F to GST-Ddlc-1. GST-Ddlc1 and Spn-F were mixed with glutathione-sepharose 4B resins. As a negative control, GST-conjugated resins were incubated with Spn-F. (Lanes 1-3) Input proteins: GST (lane 1), GST-Ddlc (lane 2) and His-Spn-F (lane 3). (Lane 4) GST-Ddlc and Spn-F; (lane 5) GST and Spn-F. When Ddlc-GST was pulled down, Spn-F was also precipitated (lane 4), whereas this was not the case when GST alone was pulled down (lane 5). (**F**) In vitro binding of Spn-F to GST-Ddlc. Extracts of wild-type ovaries were incubated with GST-Ddlc-1 or with GST alone, GST was pulled down, and the eluate was electrophoresed and probed with an anti-Spn-F antibody. (Lane 1) Control: GST-conjugated resins and ovarian extract. (Lane 2) GST-Ddlc and an ovarian extract. Spn-F associates directly with Dynein light chain in vitro. (Lane 3) Control: ovarian extract only.

We also investigated the in vitro binding of recombinant Ddlc-1 to Spn-F using pull-down assays (Fig. 6F). We incubated a fusion protein containing glutathione-S-transferase (GST) and Ddlc-1 with extracts from wild-type ovaries and precipitated the fusion protein with GSH-agarose. Co-precipitated Spn-F protein was then detected by western blot analysis. Spn-F could be co-precipitated with GST-Ddlc-1 (Fig. 6F, lane 3), but not with GST protein alone (Fig. 6F, lane 1), or with any of the other GST fusion proteins tested (data not shown). These results indicate that the Spn-F interacts specifically with Ddlc-1.

To test whether Spn-F localization to the minus end of the anterior of the oocyte is dependent on Dynein, we studied the localization of Spn-F in *Dynein heavy chain* (*Dhc64*) mutants. We tested the localization of Spn-F in hypomorphic semi-viable *dhc* allelic combinations (Gepner et al., 1996) and found that, in 70% of the egg chambers, Spn-F protein was not localized to the anterior minus end of the oocyte (Fig. 6D), and a more punctate distribution of Spn-F was found in the nurse cells. These results, together with the direct interaction of Spn-F with Dynein light chains, suggest that Spn-F transport from the nurse cells to the oocyte anterior is dependent on the minus end-directed motor Dynein.

DISCUSSION

Mutations in *spn-F* cause specific patterning defects during oogenesis, resulting in eggs and embryos that show variable alterations along the DV and AP axes. We have demonstrated that *grk* mRNA is mislocalized to the anterior circumference of the oocyte in late-stage egg chambers, instead of accumulating in the dorsoanterior region above the oocyte nucleus. The mislocalized mRNA is not translated efficiently, resulting in reduced levels of Grk in the oocyte. The decrease in Grk protein explains the ventralized eggshell and embryo phenotypes produced by *spn-F* mutations. Previous studies have indicated that *grk* is translationally repressed when not localized and is specifically derepressed at its site of localization in the dorsoanterior corner of the oocyte (Hawkins et al., 1997; Saunders and Cohen, 1999; Norvell et al., 1999). In mutations of *squid*, which encodes an hnRNP, the mislocalized *grk* mRNA along the anterior ring is translated, suggesting that Sqd protein is involved in *grk* mRNA localization and translation regulation (Norvell et al., 1999). Although our results indicate that Spn-F is also involved in *grk* mRNA localization, in *spn-F*, the mislocalized *grk* mRNA is not relieved from its translational repression.

We also observed a small fraction of *bicaudal* embryos, indicating that there was a problem with anterior posterior pattern formation; however, we did not observe ectopic Oskar protein at the anterior end of *spn-F* mutant oocytes, as might be expected, given the *bicaudal* phenotype. We did observe a minor mislocalization of Oskar protein at the posterior, which might have arisen as a result of the abnormalities in the MT or actin cytoskeleton, but this minor mislocalization cannot be the cause of the *bicaudal* phenotype. Given that only a small percentage of the embryos show the AP

patterning abnormalities, it is likely that there is a small amount of ectopic Oskar protein present at the anterior in a few egg chambers that was not detected in our experiments.

What is the mechanism by which *spn-F* affects *grk* mRNA localization? Various lines of evidence have suggested that there are two separable steps in the localization of *grk* RNA. Mutations in several genes, such as *squid* and *fs(1)K10*, allow the accumulation of *grk* RNA at the anterior, but interfere with the localization to the dorsal corner (Serano and Cohen, 1995; Neuman-Silberberg and Schüpbach, 1993; Norvell et al., 1999). Furthermore, after injection of labeled *grk* RNA into live oocytes, it was observed that *grk* mRNA particles move in two distinct steps, which are likely to involve two distinct arrays of MTs. Initially the particles move towards the anterior, subsequently they turn and move dorsally towards the oocyte nucleus (MacDougall et al., 2003). Both steps of *grk* mRNA localization require intact MTs and cytoplasmic Dynein (MacDougall et al., 2003). We have analyzed the organization and polarity of MTs in *spn-F* mutant oocytes through the imaging of Tau-GFP α-tubulin and Nod:β-gal. We detected an abnormal accumulation of GFP-Tau protein and tubulin in the periphery of the oocyte nucleus. We also tested the accumulation of Nod:β-gal, which is localized to the MT minus end during early and mid-oogenesis in wild-type oocytes. We observed that this accumulation does not occur in *spn-F* egg-chambers. However, a number of probes that normally associate with the anterior cortex of the oocyte in a MT-dependent manner, such as *bicoid* RNA and Centrosomin, appeared unaffected in *spn-F* mutants. It is possible that molecules whose anchoring at the anterior cortex is stabilized by interaction with other molecules (Pokrywka and Stephenson, 1995; Schnorrer et al., 2000) may accumulate seemingly normally at the anterior, whereas molecules that depend solely on the MT network (Nod:β-gal) are more strongly affected in the *spn-F* mutant. It may be significant that *grk* RNA itself, while localizing to the anterior, only forms a broad and fuzzy ring at the anterior of *spn-F* mutants (which is different from its accumulation in mutations such as *squid*), as *grk* RNA has been shown to require continuous transport for its anchoring (MacDougall et al., 2003). In any case, the effect of *spn-F* on the organization of the minus ends that are positioned along the anterior cortex appears to be more subtle, whereas the effect on MTs around the oocyte nucleus is much more severe, resulting in a visible disorganization and clumping of the network. The effect of *spn-F* on the organization of the MT minus end in the oocyte seems to be relatively specific, as no defects in the localization of kin:β-gal to the MT plus end were observed. We also found that Spn-F protein is localized to MT minus end in the oocyte, and in a punctate form in the nurse cells. We showed that the localization to the MT minus ends requires an intact MT network and the subunit of the motor complex *Dhc*. We also observed higher Spn-F accumulation in the nurse cells after colcemid treatment.

Given these results, one possible interpretation would be that *spn-F* mutants affect transport toward the minus end of MTs, predominantly in the subset of MTs that are required for the transport of *grk* RNA from the anterior to the dorsal side of the oocyte towards the nucleus. The observed interaction with the Dynein light chain would support such a mechanism. Another possibility is that Spn-F has a role in the organization of the minus end of MTs, with particularly strong effects on the MT network that surrounds the oocyte nucleus. The association of Spn-F with the Dynein light chain might be only transient under this model. Finally, given the collapsed aspect of the MT network in the vicinity of the oocyte nucleus, seen in the mutant egg chambers, it is also possible that Spn-F functions to provide a stabilizing connection between the minus ends of MTs and the actin cytoskeleton. However, to gain more insight into the direct role of Spn-F in MT organization, further experiments are needed. Analyzing the role of MT polymerization, MT polarity, and identifying further interaction partners of Spn-F will provide further insight into the function of the Spn-F protein.

In addition to the effects on the oocyte, we have found that *spn-F* affects the development of the bristles. The highly elongated bristles of *Drosophila* have proven to be a valuable model system for studying cellular morphogenesis. Developing bristles in *Drosophila* pupae contain 7-11 bundles of crosslinked actin filaments and a large population of MTs. During bristle growth, the rate of cell elongation increases with bristle length. It has been suggested that actin filaments and MTs play different roles during bristle elongation in *Drosophila* (Tilney et al., 2000). Whereas actin assembly is crucial for bristle cell elongation, MTs must provide other functions, such as providing bulk to the bristle cytoplasm, as well as playing a role in vesicle transport. It has also been shown that MT antagonists such as vinblastine and colchicine resulted in a decreased axial length and a compensatory increase in width, so that the volume of the bristle was not significantly changed (Fei et al., 2002). These data suggest that the MT cytoskeleton is of central importance for growth to be polarized in the axial direction (Fei et al., 2002). Mutations in the *Dynein heavy chain* resulted in shorter and thicker bristles (Gepner et al., 1996); mutations in *kinesin* also resulted in shorter and thicker bristles, and the tips of bristles were often contorted, exhibiting flattened, flared or twisted tips (Brendza et al., 2000). Although the *spn-F* bristle phenotype is comparable to the kinesin mutant bristles, the *spn-F* bristle phenotype is nevertheless unique, suggesting a specific role in the process that is slightly different from that of either Dynein or Kinesin.

In a global two-hybrid screen, Spn-F (CG12114) was found to interact with the Ik2 (CG2615) protein (Giot et al., 2003). Mutations in this protein have been isolated and characterized by Shapiro and Anderson (Shapiro and Anderson, 2006). Interestingly, *ik2* mutants share many phenotypes with *spn-F*, including a very similar bristle phenotype and specific effects on MT organization in oogenesis. However, *ik2* mutants are lethal, whereas *spn-F* homozygotes survive. In addition, whereas *spnF* mutations have only mild effects on Oskar protein localization and a low frequency of bicaudal phenotypes, such effects are more pronounced in the *ik2* mutants. Nevertheless, the striking similarities strongly suggest that the two genes function in a common pathway that affects certain types of MT more strongly than others. In normal mitotic cells, the minus ends of MTs are usually focused by the centrosomes in the interior of the cell, and plus ends contact the cortex. However, in specialized cells, such as the Drosophila oocyte, there are minus ends that make contact with the cortex (Cha et al., 2002). It is therefore possible that Spn-F and Ik2 are required for providing a stable connection between such cortical MT minus ends and cortical actin for subsets of MTs involved in specialized transport processes. Future experiments will address the interactions of Spn-F and Ik2 directly, and will determine whether, for instance, Spn-F might be a target of Ik2.

We thank Natalie Denef, Kristina Wehr and Gail Barcelo for help with ovary staining procedures. Thomas Kaufman, Paul MacDonald, Ira Clark, the Szeged Stock Center and the Bloomington Stock Center generously provided fly strains and reagents. We acknowledge Kathryn Anderson and Risa Shapiro for sharing unpublished results. We thank Jennifer Goodrich, Andrew Swan and Natalie Denef for comments on the manuscript, and the members of the Schüpbach lab for helpful discussions of the project. This work was supported by the Howard Hughes Medical Institute and by NIH grant PO1 CA41086 to T.S., and by start-up funds from Ben-Gurion University to U.A.

References

Abdu, U., Brodsky, M. and Schüpbach, T. (2002). Activation of a meiotic checkpoint during *Drosophila* oogenesis regulates the translation of Gurken through Chk2/Mnk. *Curr. Biol.* **12**, 1645-1651.

Abdu, U., Ghabrial, A., Gonzalez-Reyes, A. and Schüpbach, T. (2003). The *Drosophila spn-D* gene encodes a RAD51C-like protein that is required exclusively during meiosis. *Genetics* **165**, 197-204.

Brendza, R. P., Sheehan, K. B., Turner, F. R. and Saxton, W. M. (2000). Clonal tests of conventional kinesin function during cell proliferation and differentiation. *Mol. Biol. Cell* **11**, 1329-1343.

Brendza, R. P., Serbus, L. R., Saxton, W. M. and Duffy, J. B. (2002). Posterior localization of dynein and dorsal-ventral axis formation depends on kinesin in *Drosophila* oocytes. *Curr. Biol.* **12**, 1541-1545.

Cha, B.-J., Serbus, L. R., Koppetsch, B. S. and Theurkauf, W. E. (2002). Kinesin I-dependent cortical exclusion restricts pole plasm to the oocyte posterior. *Nat. Cell Biol.* **4**, 592-598.

Chou, T. B. and Perrimon, N. (1992). Use of a yeast site-specific recombinase to produce female germline chimeras in *Drosophila*. *Genetics* **131**, 643-653.

Clark, I. E., Jan, L. Y. and Jan, Y. N. (1997). Reciprocal localization of Nod and kinesin fusion proteins indicates microtubule polarity in the *Drosophila* oocyte, epithelium, neuron and muscle. *Development* **124**, 461-470.

Deak, P., Omar, M. M., Saunders, R. D., Pal, M., Komonyi, O., Szidonya, J., Maroy, P., Zhang, Y., Ashburner, M., Benos, P. et al. (1997). P-element insertion alleles of essential genes on the third chromosome of *Drosophila* melanogaster: correlation of physical and cytogenetic maps in chromosomal region 86E-87F. *Genetics* **147**, 1697-1722.

Fei, X., He, B. and Adler, P. N. (2002). The growth of *Drosophila* bristles and laterals is not restricted to the tip or base. *J. Cell Sci.* **115**, 3797-3806.

Gepner, J., Li, M., Ludmann, S., Kortas, C., Boylan, K., Iyadurai, S. J., McGrail, M. and Hays, T. S. (1996). Cytoplasmic dynein function is essential in *Drosophila melanogaster*. *Genetics* **142**, 865-878.

Ghabrial, A. and Schüpbach, T. (1999). Activation of a meiotic checkpoint regulates translation of Gurken during *Drosophila* oogenesis. *Nat. Cell Biol.* **1**, 354-357.

Ghabrial, A., Ray, R. P. and Schüpbach, T. (1998). *okra* and *spindle-B* encode components of the RAD52 DNA repair pathway and affect meiosis and patterning in *Drosophila* oogenesis. *Genes Dev.* **12**, 2711-2723.

Giot, L., Bader, J. S., Brouwer, C., Chaudhuri, A., Kuang, B., Li, Y., Hao, Y. L., Ooi, C. E., Godwin, B., Vitols, E. et al. (2003). A protein interaction map of *Drosophila melanogaster*. *Science* **302**, 1727-1736.

Gonzalez-Reyes, A., Elliott, H. and St Johnston, D. (1995). Polarization of both major body axes in *Drosophila* by gurken-torpedo signalling. *Nature* **375**, 654-658.

Gonzalez-Reyes, A., Elliott, H. and St Johnston, D. (1997). Oocyte determination and the origin of polarity in *Drosophila*: the role of the spindle genes. *Development* **124**, 4927-4937.

Hawkins, N. C., Van Buskirk, C., Grossniklaus, U. and Schüpbach, T. (1997). Post-transcriptional regulation of *gurken* by *encore* is required for axis determination in *Drosophila*. *Development* **124**, 4801-4810.

Heuer, J. G., Li, K. and Kaufman, T. C. (1995). The *Drosophila* homeotic target gene centrosomin (cnn) encodes a novel centrosomal protein with leucine zippers and maps to a genomic region required for midgut morphogenesis. *Development* **121**, 3861-3876.

Januschke, J., Gervais, L., Dass, S., Kaltschmidt, J. A., Lopez-Schier, H., St Johnston, D., Brand, A. H., Roth, S. and Guichet, A. (2002). Polar transport in the *Drosophila* oocyte requires Dynein and Kinesin I cooperation. *Curr. Biol.* **12**, 1971-1981.

Januschke, J., Gervais, L., Gillet, L., Keryer, G., Bornens, M. and Guichet, A. (2006). The centrosome-nucleus complex and microtubule organization in the Drosophila oocyte. *Development* **133**, 129-139.

Kammermeyer, K. L. and Wadsworth, S. C. (1987). Expression of *Drosophila* epidermal growth factor receptor homologue in mitotic cell populations. *Development* **100**, 201-210.

Li, K. and Kaufman, T. C. (1996). The homeotic target gene centrosomin encodes an essential centrosomal component. *Cell* **85**, 585-596.

Lindsley, D. L. and Zimm, G. G. (1992). *The Genome of* Drosophila melanogaster. New York: Academic Press.

MacDougall, N., Clark, A., MacDougall, E. and Davis, I. (2003). *Drosophila* gurken (TGFalpha) mRNA localizes as particles that move within the oocyte in two dynein-dependent steps. *Dev. Cell* **4**, 307-319.

Micklem, D. R., Dasgupta, R., Elliott, H., Gergely, F., Davidson, C., Brand, A., Gonzalez-Reyes, A. and St Johnston, D. (1997). The *mago nashi* gene is required for the polarisation of the oocyte and the formation of perpendicular axes in *Drosophila*. *Curr. Biol.* **7**, 468-478.

Neuman-Silberberg, F. S. and Schüpbach, T. (1993). The *Drosophila* dorsoventral patterning gene *gurken* produces a dorsally localized RNA and encodes a TGF alpha-like protein. *Cell* **75**, 165-174.

Neuman-Silberberg, F. S. and Schüpbach, T. (1996). The *Drosophila* TGF-alpha-like protein Gurken: expression and cellular localization during *Drosophila* oogenesis. *Mech. Dev.* **59**, 105-113.

Nilson, L. A. and Schüpbach, T. (1999). EGF receptor signaling in *Drosophila* oogenesis. *Curr. Top. Dev. Biol.* **44**, 203-243.

Norvell, A., Kelley, R. L., Wehr, K. and Schüpbach, T. (1999). Specific isoforms of squid, a Drosophila hnRNP, perform distinct roles in Gurken localization during oogenesis. *Genes Dev.* **13**, 864-876.

Pokrywka, N. J. and Stephenson, E. C. (1995). Microtubules are a general component of mRNA localization systems in *Drosophila* oocytes. *Dev. Biol.* **167**, 363-370.

Queenan, A. M., Barcelo, G., Van Buskirk, C. and Schüpbach, T. (1999). The transmembrane region of Gurken is not required for biological activity, but is necessary for transport to the oocyte membrane in *Drosophila*. *Mech. Dev.* **89**, 35-42.

Roth, S. and Schüpbach, T. (1994). The relationship between ovarian and embryonic dorsoventral patterning in *Drosophila*. *Development* **120**, 2245-2257.

Roth, S., Neuman-Silberberg, F. S., Barcelo, G. and Schüpbach, T. (1995). *cornichon* and the EGF receptor signaling process are necessary for both anterior-posterior and dorsal-ventral pattern formation in *Drosophila*. *Cell* **81**, 967-978.

Ruohola-Baker, H., Jan, L. Y. and Jan, Y. N. (1994). The role of gene cassettes in axis formation during *Drosophila* oogenesis. *Trends Genet.* **10**, 89-94.

Sambrook, J., Fritsch, E. F. and Maniatis, T. (1989). *Molecular cloning: A Laboratory Manual.* Cold Spring Harbor, NY: Cold Spring Harbor Laboratory Press.

Sapir, A., Schweitzer, R. and Shilo, B. Z. (1998). Sequential activation of the EGF receptor pathway during *Drosophila* oogenesis establishes the dorsoventral axis. *Development* **125**, 191-200.

Saunders, C. and Cohen, R. S. (1999). The role of oocyte transcription, the 5′UTR, and translation repression and derepression in *Drosophila gurken*. *Mol. Cell* **3**, 43-54.

Schnorrer, F., Bohmann, K. and Nusslein-Volhard, C. (2000). The molecular motor dynein is involved in targeting swallow and *bicoid* RNA to the anterior pole of *Drosophila* oocytes. *Nat. Cell Biol.* **2**, 185-190.

Schnorrer, F., Luschnig, S., Koch, I. and Nusslein-Volhard, C. (2002). Gamma-tubulin37C and gamma-tubulin ring complex protein 75 are essential for *bicoid* RNA localization during *Drosophila* oogenesis. *Dev. Cell* **3**, 685-696.

Schüpbach, T. (1987). Germ line and soma cooperate during oogenesis to establish the dorsoventral pattern of egg shell and embryo in *Drosophila melanogaster*. *Cell* **49**, 699-707.

Serano, T. L. and Cohen, R. S. (1995). A small predicted stem-loop structure mediates oocyte localization of *Drosophila K10* mRNA. *Development* **121**, 3809-3818.

Shapiro, R. S. and Anderson, K. V. (2006). *Drosophila* Ik2, a member of the IκB kinase family, is required for mRNA localization during oogenesis. *Development* **133**, 1467-1475.

Spradling, A. C. and Rubin, G. M. (1982). Transposition of cloned P elements into *Drosophila* germ line chromosomes. *Science* **218**, 341-347.

Staeva-Vieira, E., Yoo, S. and Lehmann, R. (2003). An essential role of DmRad51/SpnA in DNA repair and meiotic checkpoint control. *EMBO J.* **22**, 5863-5874.

Tearle, R. and Nüsslein-Volhard, C. (1987). Tübingen mutants stock list. *Dros. Inf. Serv.* **66**, 209-226.

Tilney, L. G., Connelly, P. S., Vranich, K. A., Shaw, M. K. and Guild, G. M. (2000). Actin filaments and microtubules play different roles during bristle elongation in *Drosophila*. *J. Cell Sci.* **113**, 1255-1265.

Van Doren, M., Williamson, A. L. and Lehmann, R. (1998). Regulation of zygotic gene expression in *Drosophila* primordial germ cells. *Curr. Biol.* **8**, 243-246.